Wind Energy Conversion Systems with Integrated Active Filter Capabilities Using DFIG and Control by Using Fuzzy

S. Vaishali[*], G. Goutham Reddy

PG Student, Department of EEE, JNTUA, Ananthapuramu, Andhra Pradesh, India

ABSTRACT

This paper proposes the operation of doubly fed induction generator (DFIG) with integrated active filter capabilities by using grid side converter (GSC). When the wind turbine is in shutdown condition the wind energy conversion system acts as a static compensator (STATCOM) for supplying harmonics. For supplying harmonics in addition to its slip power transfer the grid side converter plays an important role. Both gaining the maximum power extraction and to provide required reactive power to the DFIG rotor-side converter is used. Detailed control algorithms of both RSC and GSC are presented. Here we are using the fuzzy controller compared to other controllers because of its accurate performance. Implemented project DFIG- based WECS is simulated using MATLAB/Simulink.

Keywords: Doubly Fed Induction Generator (DFIG), Integrated Active Filter, Power Quality, Nonlinear Load, Wind Energy Conversion Systems (WECS).

I. INTRODUCTION

Now a day's nonrenewable energy resources are getting degrading and power demand also going on increasing by the increasing level of utility of power. So the renewable sources are being utilized to meet the ever increasing energy demand. Wind energy is taken into account to be one amongst the potential sources of fresh energy for the long run. Nowadays, several complete loads area unit powered by renewable supply of energy and controlling of this project is completed by using fuzzy controller.

Out of all renewable energy sources the wind energy is the most preferred because they are unlimited and eco-friendliness. In the beginning wind turbines are used as fixed speed wind turbines with squirrel cage induction generator and condenser banks. Because of their simplicity and low price fixed speed wind turbines are preferred. To extract maximum power, the machine should run at variable rotor speeds at completely different wind speeds. Using trendy power electronic converters, the machine is able to run at adjustable speeds. Doubly fed induction generators are preferred among other types due to less cost. DFIG has many more advantages like higher energy output, lower converter rating, better utilization of generators and good damping performance for the weak grid can be provided. By the decoupled vector control algorithm independent control of active and reactive power is achieved. To such system vector control is usually realized in synchronously rotating reference frame destined in either voltage axis or flux axis. Rotor-side converter (RSC) control is implemented in voltage-oriented reference system. DFIG-based wind energy

TABLE 1 : Current Distortion Limits For General Distribution Systems In Terms Of Individual Harmonics Order (Odd Harmonics)

I_{sc}/I_l	>11	$11 \leq h \leq 17$	$17 \leq h \leq 23$	$23 \leq h \leq 35$	$35 \leq h$	TDD
<20	4.0	2.0	1.5	0.6	0.3	5.0
20<50	7.0	3.5	2.5	1.0	0.5	8.0
50<100	10	4.5	4.0	1.5	0.7	12
100<1000	12	5.5	5.0	2.0	1.0	15.0
>1000	15.0	7.0	6.0	2.5	1.4	20.0

Maximum harmonic current distortion is in percent of I_L.
I_{SC} = maximum short-circuit current at PCC.
I_L = maximum demand load current (fundamental frequency component) at PCC.

Conversion system (WECS) reaction to grid disturbance is compared to the fixed speed WECS. In the grid wind penetration becomes important the variable speed WECS are utilized for smoothening of power and harmonic mitigation additionally to its power generation. By using super magnetic energy storage systems this power smoothening is achieved. Both transient stability limit and reactive power requirement are achieved by static compensator (STATCOM).

A distribution STATCOM (DSTATCOM) let alone fly-wheel energy storage system is employed at the wind farm for mitigating frequency disturbances and harmonics. For mitigating the power quality issues and reactive power compensation researches have changed the control algorithms of already existed DFIG converters.

By using RSC reactive power control and harmonics compensation is obtained. Thus, from the RSC harmonics are injected in to the rotor windings, which lead to losses and noise in the machine. These totally different harmonics in rotating part may also produce mechanical unbalance. Due to these methods RSC rating increases. By using GSC harmonic compensation and reactive power control are done. Because of this harmonics cannot pass through machine windings in all these cases.

In this work, an indirect current control is used for compensating harmonics produced by nonlinear loads. Reactive power control of DFIG is done by RSC. PWM pulses are generated without any error by exploitation the fuzzy controller. The main advantage of planned DFIG is that it works as an energetic filter even once the turbine is in shutdown condition. Hence it compensates load reactive power and harmonics at turbine stall case. At varied wind speeds planned DFIG's dynamic performance is also demonstrated.

II. METHODS AND MATERIAL

1. System Configuration and Operating Principle

In DFIG, the stator coil is directly connected to the grid as shown in Fig.1. Fig.1 shows a schematic diagram of the planned DFIG primarily based WECS with integrated active filter capabilities. At PCC nonlinear loads are connected. Between grid and the rotor two back-to-back voltage source converters (VSCs) are

placed. The planned DFIG operates as an active filter additionally to the active power generation similar to traditional DFIG. The PCC voltage gets distorted by the harmonics which are produced by the nonlinear loads at the PCC. By the GSC control these nonlinear load harmonic currents are reduced, thus the stator coil and grid harmonic currents becomes harmonic free. Voltage-oriented reference frame control method is used for achieving maximum power point tracking (MPPT) and additionally for creating unity power factor at the stator coil. For extracting, the fundamental component of load currents for the GSC control synchronous reference (SRF) control methodology is used.

DESIGN OF DFIG-BASED WECS

For the operation of WECS selection of ratings of VSCs and dc-link voltage is extremely much important.

A. Selection of DC-Link Voltage

Dc-link voltage selection depends on both rotor voltage and PCC voltage. When rotor side is considered, rotor voltage is slip times the stator voltage. Here DFIG has stator to rotor turns ratio as 2:1.Generally, the operating slip of the DFIG is ± 0.3. So, the rotor voltage is always less than the PCC voltage. Hence, by considering only PCC voltage the design criteria for the selection of dc-link voltage is achieved, When GSC side is considered.
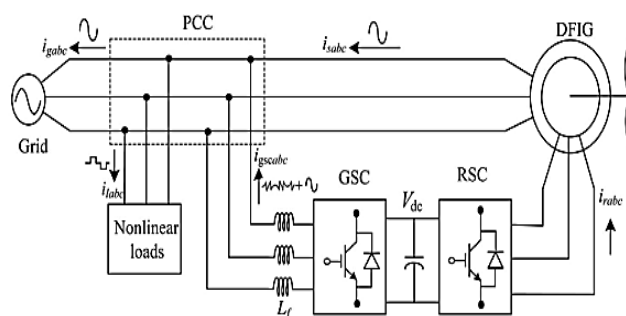

Figure 1. System Configuration

the PCC line voltage (v_{ab}) is 230v, as the machine is in delta mode. Hence the dc-link voltage is estimated as

$$v_{dc} \geq \frac{2\sqrt{2}}{\sqrt{3}*m} v_{ab} \qquad (1)$$

v_{ab}– line voltage at the PCC. For linear range maximum modulation index is selected as 1. The approximate value of dc-link voltage (v_{dc}) by (1) is 375 V. So, it is selected as 375V.

a. Selection of VSC Rating

The lagging volt-ampere reactive (VAR) was draws by DFIG for its excitation to build the rated air gap voltage. DFIG requires lagging VAR of 2 KVAR when it is running as a motor. The operating speed range in DFIG is 0.7 to1.3 p.u. Thus the maximum slip (S_{max}) is 0.3.Reactive power of 600 VAR (S_{max}* Q_s =0.3 *2KVAR) is required from the rotor side (Q_{rmax}) to make unity power factor at the stator side. Maximum rotor active power is(S_{max}* P) and the power rating of the DFIG is 5 KW. Thus, the maximum rotor active power (P_{rmax}) is 1.5 kW (0.3 * 5 kW = 1.5 kW) So, the rating of the VSC used as RSC S_{rated} is given as

$$S_{rated} = \sqrt{P_{rmax}^2 + Q_{rmax}^2} \qquad (2)$$

Thus, S_{rated} =1.615 KVA.

C. Design of Interfacing Inductor

Interfacing inductors between GSC and PCC depends on the allowable GSC current limit (i_{gscpp}), dc-link voltage, and switching frequency of GSC. For calculation maximum possible GSC line currents are used and these line currents depend upon the line voltage and maximum power at GSC. In GSC slip power is the maximum possible power and here the slip power is 1.5 KW. At GSC Line voltage (V_L) is 230 V. Then, the line current is obtained as I_{gsc}= 1.5 kW/($\sqrt{3}$ * 230) = 3.765A. The peak ripple current considered as 25% of rated GSC current, the inductor value is calculated as

$$L_i = \frac{\sqrt{3}mv_{dc}}{12af_m\Delta i_{gsc}} \qquad (3)$$

The value of an Interfacing inductor is selected as 4 mH.

2. Control Strategy And Simulation Results

For both GSC and RSC control algorithms are presented here and complete control schematic is shown is Fig.2. The control algorithm for emulating wind turbine characteristics using dc machine and Type A chopper is also shown.

A. Control of RSC

To extract maximum power for a particular wind speed direct axis reference rotor current is selected and this can be achieved by running the DFIG at a rotor speed for a particular wind speed. The direct axis reference rotor current (i_{dr}^*) is

$$i_{dr}^* (k) = i_{dr}^* (k-1) + k_{pd}\{\omega_{er}(k) - \omega_{er}(k-1)\} + k_{id}\omega_{er}(k) \qquad (4)$$
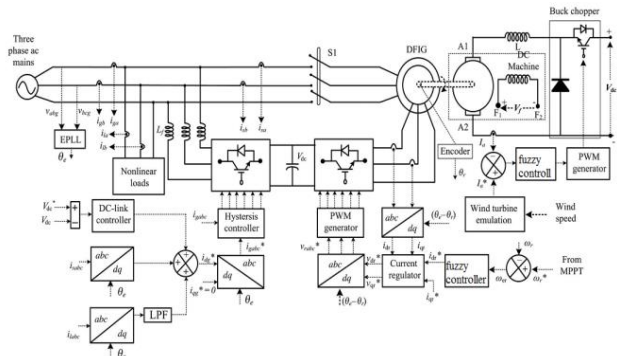

Figure 2. Control algorithm of the WECS

To obtain speed error (ω_{er}) subtract sensed speed (ω_r)from the reference speed (ω_r^*). Where k_{id} and k_{pd} are the integral and proportional constants of speed controller. $\omega_{er}(k)$ and $\omega_{er}(k-1)$ are the speed errors at kth and (k-1)th instants. $i_{dr}(k)$ and $i_{dr}(k-1)$ are the direct axis reference rotor currents at kth and (k-1)th instants. For a particular wind speed reference rotor speed (ω_r^*) is estimated by optimal tip speed ratio control.

By controlling direct and quadrature axis rotor currents (i_{dr} and i_{qr}) active and reactive powers are controlled. The sensed rotor currents (i_{ra}, i_{rb}, and i_{rc}) are used to calculate i_{dr} and i_{qr} currents.

$$i_{dr} = \frac{2}{3}\left[i_{ra}\sin\theta_{slip} + i_{rb}\sin(\theta_{slip} - \frac{2\pi}{3}) + i_{rc}\sin(\theta_{slip} + \frac{2\pi}{3})\right] \qquad (5)$$

$$i_{qr} = \frac{2}{3}\left[i_{ra}\cos\theta_{slip} + i_{rb}\cos(\theta_{slip} - \frac{2\pi}{3}) + i_{rc}\cos(\theta_{slip} + \frac{2\pi}{3})\right] \qquad (6)$$

Slip angle (θ_{slip}) is $\theta_{slip} = \theta_e - \theta_r$ $\qquad (7)$

For aligning rotor currents into voltage axis, θ_e is calculated from PLL. Encoder is used to achieve rotor position θ_r.

Direct and quadrature axis rotor voltages (v'_{dr} and v'_{qr}) are obtained from direct and quadrature axis rotor current errors (i_{der} and i_{qer}) as

$$v'_{dr}(k) = v'_{dr}(k-1) + k_{pdv}\{i_{der}(k) - i_{der}(k-1)\}$$
$$+ k_{idv}i_{der}(k) \tag{8}$$

$$v'_{qr}(k) = v'_{qr}(k-1) + k_{pqv}\{i_{qer}(k) - i_{qer}(k-1)\}$$
$$+ k_{iqv}i_{qer}(k) \tag{9}$$

Where k_{pdv} and k_{idv} are the proportional and integral gains of direct axis current controller. By adding some compensating terms direct and quadrature components are decoupled as

$$v^*_{dr} = v'_{dr} + (\omega_e - \omega_r)\sigma L_r i_{qr} \tag{10}$$

$$v^*_{qr} = v'_{qr} - (\omega_e - \omega_r)(L_m i_{ms} + \sigma L_r i_{dr}) \tag{11}$$

Reference direct and quadrature voltages(v^*_{dr} ,v^*_{qr}) are converted into three phase reference rotor voltages (v^*_{ra} ,v^*_{rb} ,v^*_{rc}) as

$$v^*_{ra} = v^*_{dr}\sin\theta_{slip} + v^*_{qr}\cos\theta_{slip} \tag{12}$$

$$v^*_{rb} = v^*_{dr}\sin(\theta_{slip} - 2\pi/3) + v^*_{qr}\cos(\theta_{slip} - 2\pi/3) \tag{13}$$

$$v^*_{rc} = v^*_{dr}\sin(\theta_{slip} + 2\pi/3) + v^*_{qr}\cos(\theta_{slip} + 2\pi/3) \tag{14}$$

To generate pulse-width modulation (PWM) signals for the RSC these three phase rotor reference voltages (v^*_{ra} ,v^*_{rb} ,v^*_{rc}) are compared with triangular carrier wave of fixed switching frequency.

By using Ziegler Nicholas method tuning of Fuzzy controllers which are used in both RSC and GSC can be achieved.

Generally, the quadrature axis reference rotor current (i^*_{qr}) is selected such that the stator reactive power (Q_s) is made zero. To inject the required reactive power, quadrature axis reference rotor current (i^*_{qr}) is selected.

B. Control of GSC

GSC is controlled for mitigating the harmonics produced by nonlinear loads.

For making grid currents sinusoidal and balanced, an indirect current control is applied on the grid currents. To make grid currents sinusoidal and balanced this GSC supplies the harmonics. By processing the dc-link voltage error (v_{dce}) between reference and estimated dc-link voltage (V^*_{dc} and V_{dc}) through Fuzzy controller active power component of GSC current is obtained as

$$i^*_{gsc}(k) = i^*_{gsc}(k-1) + k_{pdc}\{v_{dce}(k) - v_{dce}(k-1)\} + k_{idc}v_{dce}(k) \tag{15}$$

Where k_{pdc} and k_{idc} are proportional and integral gains of dc-link voltage controller. $V_{dce}(k)$ and $V_{dce}(k-1)$ are dc-link voltage errors at kth and (k-1) instants. $i^*_{gsc}(k)$ and $i^*_{gsc}(k-1)$ are active power component of GSC current at kth and (k-1)th instants.

Using abc to dq transformation, active power component of stator current (i_{ds}) is obtained from the sensed stator currents (i_{sa}, i_{sb}, and i_{sc}) as

$$i_{ds} = 2/3\left[i_{sa}\sin\theta_e + i_{sb}\sin(\theta_e - 2\pi/3) + i_{sc}\sin(\theta_e + 2\pi/3)\right] \tag{16}$$

Using SRF theory fundamental active load current ($\overline{i_{ld}}$) is obtained. To convert the load currents in to synchronously rotating dq frame ($\overline{\overline{i_{ld}}}$) the value of phase angle from EPLL and the instantaneous load currents (i_{labc}) are used. In synchronously rotating dq frame ($\overline{i_{ld}}$) DC values of load currents are extracted using low-pass filter (LPF).

From the direct axis current of stator current (i_{ds}) and load current ($\overline{i_{ld}}$) in synchronously rotating frame and the loss component of GSC current (i^*_{gsc}), direct axis component of reference grid current (i^*_{gd}) is achieved and given as

$$i^*_{gd} = i^*_{gsc} + i_{ds} - \overline{i_{ld}} \tag{17}$$

To avoid dragging of any reactive power from grid, quadrature axis component of reference grid current (i^*_{gq}) is selected as zero.

To generate switching pulses for the GSC hysteresis current controller is used which is a feedback current controller where sensed current tracks the reference current within a hysteresis band (i_{hb}). At each sampling instant, the actual current (i_{gabc}) is compared to the reference current (i^*_{gabc}) as

$$\Delta i_{gabc} = i^*_{gabc} - i_{gabc} \quad (18)$$

When $\Delta i_{gabc} > i_{hb}$, lower switch is turned ON $\quad$ (19)

When $\Delta i_{gabc} < -i_{hb}$, upper switch is turned ON $\quad$ (20)

In similar way using these equations, gating pulses for three phases of GSC are generated.

3. Fuzzy Logic Controller

In FLC, the complete control action is determined by a set of linguistic rules. The advantage of fuzzy control is that it is based on a linguistic description and does not require a mathematical model of the system.
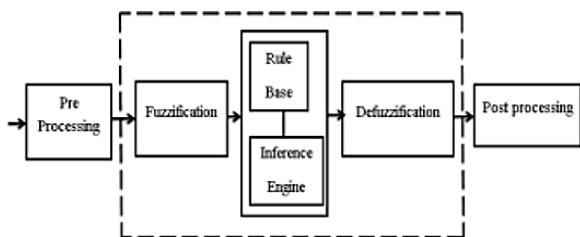
Figure 3. Fuzzy Logic Controller

Fuzzy logic controller (FLC) shown in fig.3 consists of fuzzification block (done by transferring input (crisp) sets in to fuzzy sets), inference system (rules are framed) and defuzzification block (to provide specific outputs). Seven membership functions are used for error; change in error and also for controller output. Triangular membership function is used in the design of fuzzy controller.

Table II: Fuzzy Rules

Change in error	Error						
	NB	NM	NS	ZE	PS	PM	PB
NB	NB	NB	NB	NB	NM	NS	ZE
NM	NB	NB	NB	NM	NS	ZE	ZE
NS	NB	NB	NM	NS	ZE	PS	PM
ZE	NB	NM	NS	ZE	PS	PM	PB
PS	NM	NS	ZE	PS	PM	PB	PB
PM	NS	ZE	PS	PM	PB	PB	PB
PB	ZE	PS	PM	PB	PB	PB	PB

Fuzzification: Using seven fuzzy subsets membership function values are assigned to the linguistic variables. The notation of the membership function are Negative Big (NB), Negative Medium (NM), Negative Small (NS), Zero (ZE), Positive Small (PS), Positive Medium (PM) and Positive Big (PB).
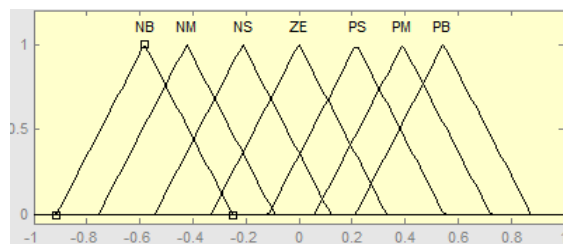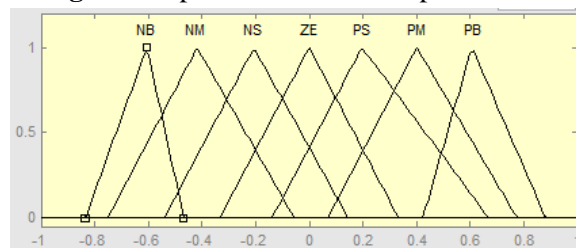

Figure 4. Input error membership functions

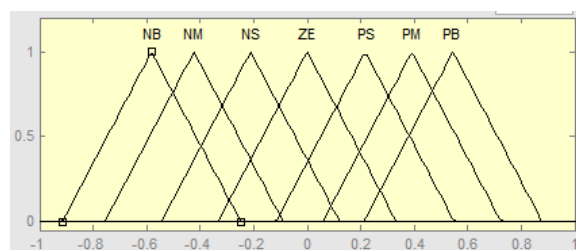**Figure 5.** Changing error as input membership functions

Figure 6. Output variable membership functions

Inference Method: In the literature various methods have been presented like Max-Min and Max-Dot and here Min method is used.

Defuzzificztion: The basic operation of Fuzzy logic controller (FLC) is constructed from fuzzy control rules utilizing the values of fuzzy sets in general for the error and the change of error and control action. The results are combined to give a crisp output controlling the output variable and this process is called as "Defuzzification".

The set of FC rules are derived from
$$u = -[\alpha E + (1 - \alpha) * C] \quad (21)$$

Where α is self adjustable factor and it regulates the whole operation. E is the system's error. C and u are the change in error, control variable.

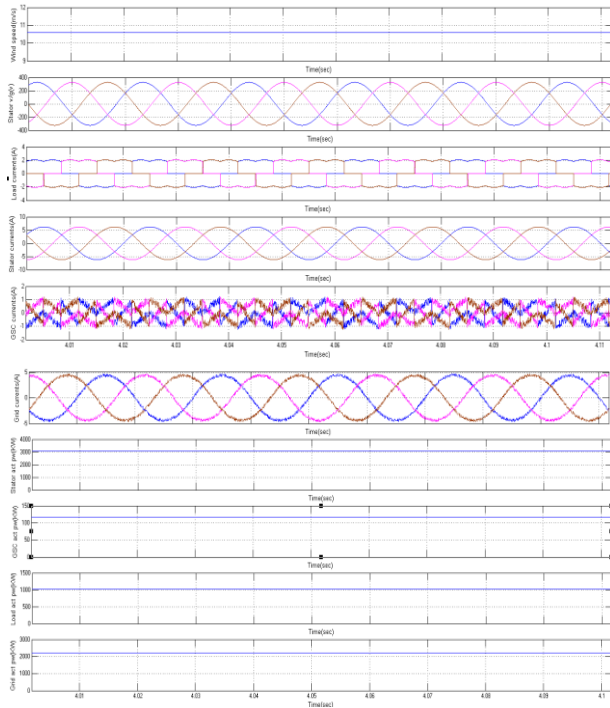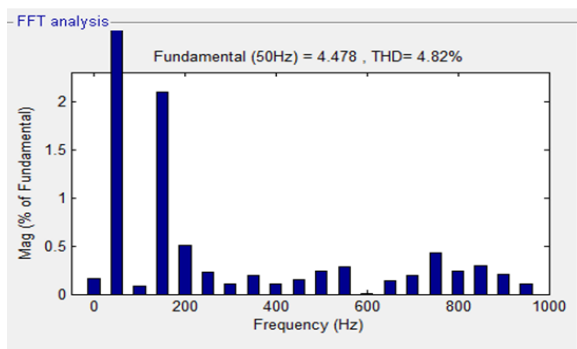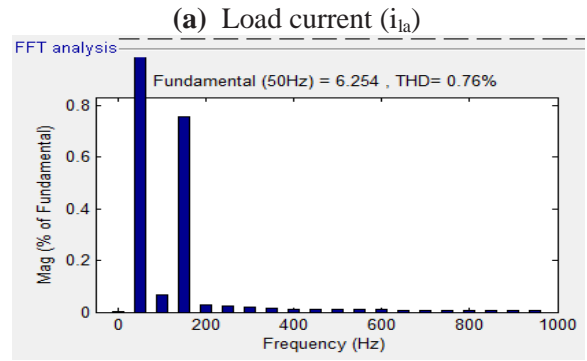## III. RESULTS AND DISCUSSION

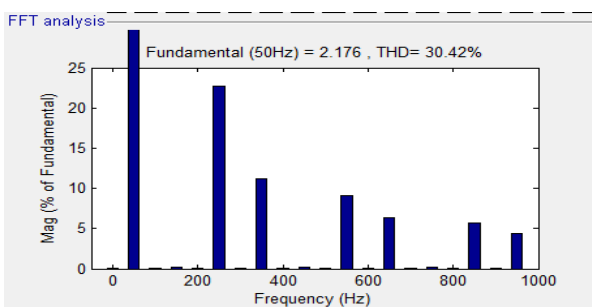**Simulation Results**

Figure 7. Simulated performance of the DFIG-based WECS at fixed wind speed of 10.6m/s (rotor speed of 1750 rpm).

Harmonic Spectra

(a) Grid current (i_{ga})

(a) Load current (i_{la})

(c) Stator current (i_{sa})
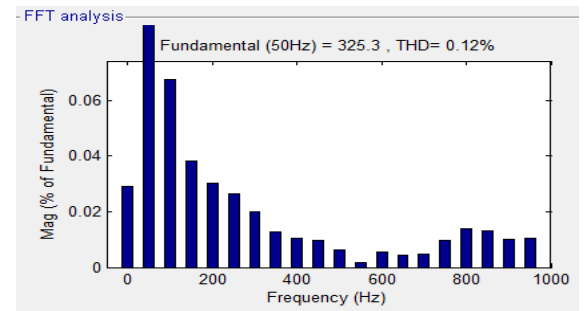
(d) Grid voltage for phase "a" (v_{ga}) at fixed wind speed of 10.6 m/s (rotor speed of 1750 rpm)
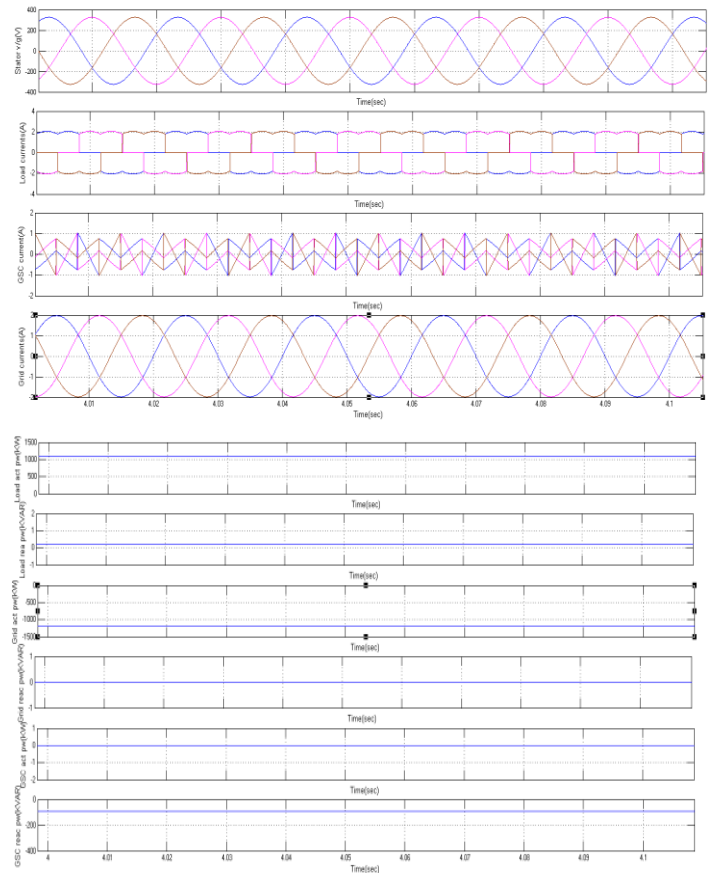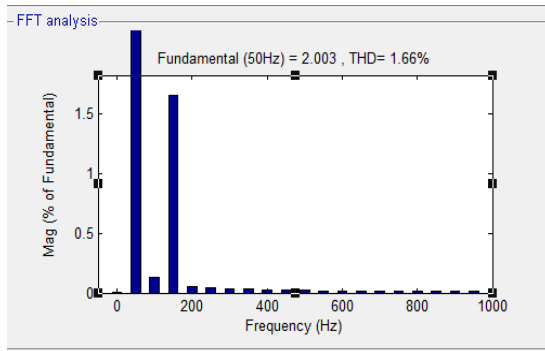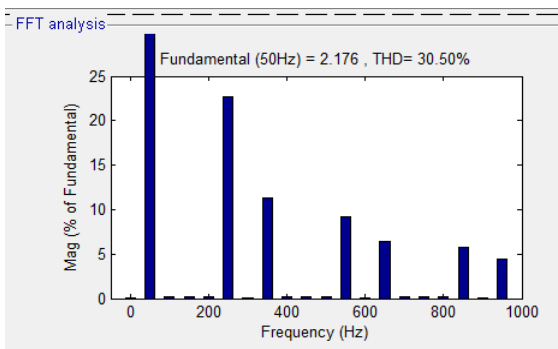

Figure 8. Simulated performance of the DFIG-based WECS working as a STATCOM at zero wind speed.

Harmonic Spectra

(a) Grid current (i_{ga})
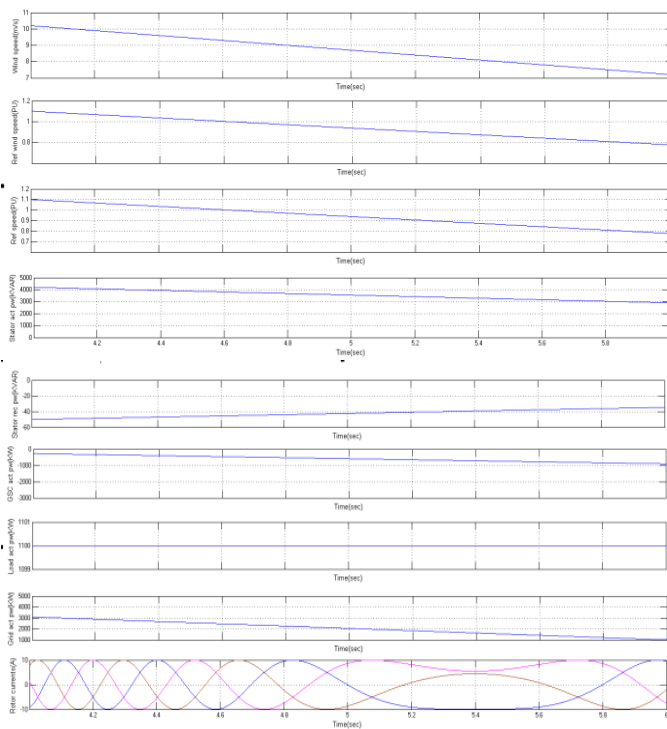

(b) Load Current (i_{la})

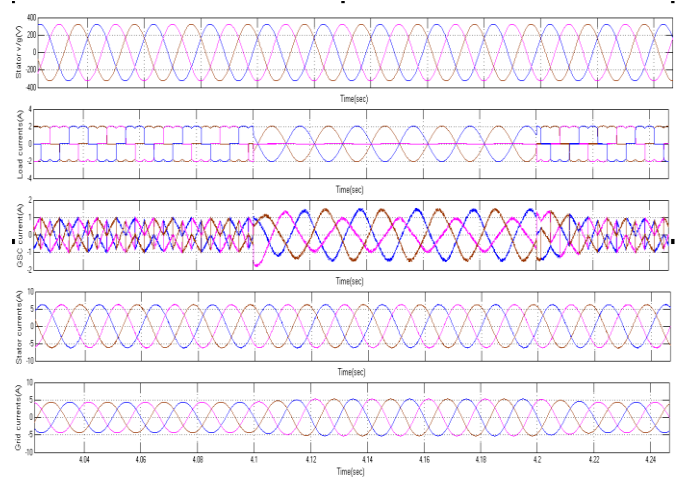**Figure 9**. Simulated performance of DFIG for fall in wind speed.

Figure 10. Dynamic performance of DFIG-based WECS for the sudden removal and application of local loads.

IV. CONCLUSION

In this project DFIG, the load reactive power has been supplied from the GSC and the reactive power for the induction machine has been provided from the RSC. The grid side device control algorithm of this DFIG has been changed for supplying the harmonics and reactive power of the local loads. Both active and reactive powers have been achieved by RSC control. The controlling for this device is completed by the fuzzy controller. The project DFIG has additionally been verified at turbine obstruction condition for compensating harmonics and reactive power of local loads. This proposed system with an integrated active filter has been simulated using MATLAB/Simulink environment. Dynamic performance of this proposed GSC control algorithm has also been verified for the variation in the wind speeds and for local nonlinear load.

V. REFERENCES

[1] D. M. Tagare, Electric Power Generation the Changing Dimensions. Piscataway, NJ, USA: IEEE Press, 2011.

[2] G. M. Joselin Herbert, S. Iniyan, and D. Amutha, "A review of technical issues on the development of wind farms," Renew. Sustain. Energy Rev., vol. 32, pp. 619–641, 2014.

[3] I. Munteanu, A. I. Bratcu, N.-A. Cutululis, and E. Ceang, Optimal Control of Wind Energy Systems Towards a Global Approach. Berlin, Germany: Springer-Verlag, 2008.

[4] A. A. B. MohdZin, H. A. Mahmoud Pesaran, A. B. Khairuddin, L. Jahanshaloo, and O. Shariati, "An overview on doubly fed induction generators controls and contributions to wind based electricity generation," Renew. Sustain. Energy Rev., vol. 27, pp. 692–708, Nov. 2013.

[5] ShilpyAgrawal, Vijay Bhuria, "Shunt active power filter for harmonic mitigation by using Fuzzy logic controller"vol 2, June 2013.

[6] S. S. Murthy, B. Singh, P. K. Goel, and S. K. Tiwari, "A comparative study of fixed speed and variable speed wind energy conversion systems feeding the grid," in Proc. IEEE Conf. Power Electron. Drive Syst. (PEDS'07), Nov. 27–30, 2007, pp. 736–743.

[7] D. S. Zinger and E. Muljadi, "Annualized wind energy improvement using variable speeds," IEEE Trans. Ind. Appl., vol. 33, no. 6, pp. 1444– 1447, Nov./Dec. 1997.

[8] H. Polinder, F. F. A. van der Pijl, G. J. de Vilder, and P. J. Tavner, "Comparison of direct-drive and geared generator concepts for wind turbines," IEEE Trans. Energy Convers., vol. 21, no. 3, pp. 725–733, Sep. 2006.

[9] R. Datta and V. T. Ranganathan, "Variable-speed wind power generation using doubly fed wound rotor induction machine—A comparison with alternative schemes," IEEE Trans. Energy Convers., vol. 17, no. 3, pp. 414–421, Sep. 2002.

[10] E. Muljadi, C. P. Butterfield, B. Parsons, and A Ellis, "Effect of variable speed wind turbine generator on stability of a weak grid," IEEE Trans. Energy Convers., vol. 22, no. 1, pp. 29–36, Mar. 2007.

[11] R. Pena, J. C. Clare, and G. M. Asher, "Doubly fed induction generator using back-to-back PWM converters and its application to variable-speed wind-energy generation," IEE Proc. Elect. Power Appl., vol. 143, no. 3, pp. 231–241, May 1996.